Bioelectrochemistry 96 (2014) 7–13

Contents lists available at ScienceDirect

Bioelectrochemistry

journal homepage: www.elsevier.com/locate/bioelechem

Ultrasensitive electrochemical aptasensor for ochratoxin A based on two-level cascaded signal amplification strategy

Xingwang Yang [1], Jing Qian [1], Ling Jiang, Yuting Yan, Kan Wang, Qian Liu, Kun Wang *

Key Laboratory of Modern Agriculture Equipment and Technology, School of Chemistry and Chemical Engineering, Jiangsu University, Zhenjiang, 212013, P.R. China

ARTICLE INFO

Article history:
Received 11 September 2013
Received in revised form 21 November 2013
Accepted 24 November 2013
Available online 4 December 2013

Keywords:
Signal amplification
Gold nanoparticle
Electrochemical
Aptasensor
Ochratoxin A

ABSTRACT

Ochratoxin A (OTA) has a number of toxic effects to both humans and animals, so developing sensitive detection method is of great importance. Herein, we describe an ultrasensitive electrochemical aptasensor for OTA based on the two-level cascaded signal amplification strategy with methylene blue (MB) as a redox indicator. In this method, capture DNA, aptamers, and reporter DNA functionalized-gold nanoparticles (GNPs) were immobilized on the electrode accordingly, where GNPs were used as the first-level signal enhancer. To receive the more sensitive response, a larger number of guanine (G)-rich DNA was bound to the GNPs' surface to provide abundant anchoring sites for MB to achieve the second-level signal amplification. By employing this novel strategy, an ~8.5 (±0.3) fold amplification in signal intensity was obtained. Afterward, OTA was added to force partial GNPs/G-rich DNA to release from the sensing interface and thus decreased the electrochemical response. An effective sensing range from 2.5 pM to 2.5 nM was received with an extremely low detection limit of 0.75 (±0.12) pM. This amplification strategy has the potential to be the main technology for aptamer-based electrochemical biosensor in a variety of fields.

1. Introduction

Ochratoxin A (OTA), a toxic fungal metabolite derived from several species of the genera Aspergillus and Penicillium, has been identified as a global contaminating mycotoxin in a wide variety of plant products such as cereals, beans, coffee and beverages like beer and wine [1,2], and may also exist in human blood and breast milk [3]. OTA is known to cause nephrotoxic, hepatotoxic, neurotoxic, teratogenic, and immunotoxic effects to both humans and animals, and has been classified as a potential carcinogen (group 2B) for human beings [4,5]. As a consequence, maximum tolerated levels of OTA have been fixed by countries around the world. For example, the European Commission has established the maximum level of OTA in food products such as raw cereal grains (12.5 nM), grape juice (7.5 nM), and the food special for infants (1.25 nM) [6–8]. Considering the serious threat from OTA, it is of great importance to develop sensitive detection method to ensure food safety issues and prevent the risk of human OTA consumption. Conventional instrument-based methods involving gas chromatography, high performance liquid chromatography and their combination to fluorescence, ultraviolet, and mass spectrometry were applied for OTA detection [9–11]. Despite their accuracy and lower detection limits, their wide use was hindered by the requirement for sophisticated equipments, complicated pre-treatments of samples, and high skilled personnel. A common alternative for OTA detection are immunoassays which depend on the antigen–antibody interactions [12–18]. For instance, enzyme-linked immunosorbent assay (ELISA) [12] and colloid gold labeled immunochromatographic strip [17] were successfully developed. Besides, antibody-based fluorescence polarization immunoassay was also constructed for rapid detection of OTA [18]. Although all above mentioned methods benefit from good sensitivity, as well as simplicity, acceptable reliability and low requirement for expensive equipments and technical skills, their application to physiological conditions is limited by the proteic nature of antibodies [19]. Note that the usage of the antibodies is of high cost because the preparation of antibodies is a time-consuming and labour-intensive process including hapten, immunogen synthesis, and the animal immunity.

Aptamers are single stranded oligonucleotides which are selected by the systematic evolution of ligands by exponential enrichment (SELEX) technique and possess high affinity and selectivity for targets that contain small molecules, proteins, and whole cells [20–22]. In contrast with antibodies, aptamers possess obvious advantages including a simpler synthesized process, a better stability for long-term storage, commercial availability, and the flexible modification with a variety of functional groups [23,24]. Since the first report of the aptamer against OTA by Cruz-Aguado and Penner in 2008 [25], different versions of aptasensors come out about the OTA determination by utilizing the specific binding between target and aptamer, based on a variety of signal transducers such as fluorescent [26–28], electrochemiluminescent

* Corresponding author. Tel.: +86 511 88791800; fax: +86 511 88791708.
E-mail address: wangkun@ujs.edu.cn (K. Wang).
[1] These authors contributed equally to this work.

1567-5394/$ – see front matter © 2013 Elsevier B.V. All rights reserved.
http://dx.doi.org/10.1016/j.bioelechem.2013.11.006

[29], and electrochemical [19,30–34]. Among them, the electrochemical methods are widely recognized to be a powerful analytical tool due to a wide variety of positive attributes such as simple instrumentation, easy operation, low cost, high sensitivity, and rapid sensing time. In order to further improve the sensitivity of the electrochemical aptasensors, various signal amplification strategies [31–37] have been proposed such as exonuclease-catalyzed target recycling amplification [32], enzyme labeling amplification [33,34], and aptamer-based rolling circle amplification [35,37]. Despite these methods offering advantages in terms of signal amplification, commercialization of these sensors might be hampered by the use of the expensive and unstable enzymes. Besides, inorganic nanoparticles can also serve as labels to amplify the signal for OTA detection, taking advantages of their high stability, low cost, and labeling convenience [38]. However, more sensitive and consistent methods are strongly desirable in the development of aptasensors for OTA detection.

Herein, a two-level cascaded signal amplification based on a sandwich model was developed: (1) gold nanoparticles (GNPs) were functionalized with reporter DNA as the first-level signal enhancer; (2) guanine (G)-rich DNA was bound to the GNPs surface as the second-level signal enhancer. An electrochemical indicator, methylene blue (MB), which mainly binds to the free guanine (G) bases by the previous studies [39,40], was used as the indicator of the hybridization events. As a result, the reduction peak of MB was a direct function of the amounts of GNPs and G-rich DNA localized at the electrode surfaces. The quantification of OTA was completed by monitoring the signal variance generated from MB on the electrode before and after the addition of OTA into the sensing system.

2. Experimental section

2.1. Apparatus

The morphology and size of the GNPs were analyzed with transmission electron microscopy (TEM) technique (JEOL 2100, JEOL, Japan). The UV-vis spectra were measured on a Perkin-Elmer Lambda 18 UV-vis-NIR spectrometer (USA). Cyclic voltammetry (CV), differential pulse voltammogram (DPV), and electrochemical impedance spectroscopy (EIS) experiments were performed on a CHI 660B workstation (CHI Instrument, China) based on a conventional three-electrode system composed of the modified Au electrode (1 mm in diameter) as the working electrode, platinum wire as the counter electrode, and saturated calomel electrode (SCE) as the reference electrode. EIS measurements were carried out under an oscillation potential of 5 mV over the frequency range of 10 kHz to 0.01 Hz at +0.20 V (vs. SCE).

2.2. Reagents

GNPs were prepared by the citrate reduction of $HAuCl_4$ according to the literature [38]. Capture DNA (DNA1): 5′-HS-TGT CCG ATG CTC-3′; aptamer (DNA2): 5′-GAT CGG GTG TGG GTG GCG TAA AGG GAG CAT CGG ACA-3′; reporter DNA (DNA3): 5′-CCA CAC CCG ATC-SH-3′; G-rich DNA (DNA4): 5′-GAT CGG GTG TGG AGG TGG CGG TGG CGG AGG TGG CGG TGG-3′ were purchased from Sangon Biotech Co., Ltd (Shanghai, China). OTA, ochratoxin B (OTB), and fumonisin B1 (FB1) were obtained from Sigma-Aldrich. 6-Mercaptohexanol (MCH), hydrogen tetrachloroaurate(III) ($HAuCl_4$), trisodium citrate, ethylenediaminetetraacetic acid disodium salt (EDTA), tris hydroxy methyl aminomethan (Tris), and MB were purchased from Sinopharm Chemical Reagent Co., Ltd (China). DNA oligonucleotide stock solutions were prepared with 50 mM Tris–HCl buffer (pH 7.0, containing 0.2 M NaCl and 1.0 mM EDTA) and kept at 4 °C in dark. All the reagents were at least of analytical grade. Double-distilled water was used throughout the study.

2.3. Conjugation of DNA3 to the gold nanoparticles

The conjugation of DNA3 to the GNPs was performed according to the literature [38]. Briefly, 2 mL of as-prepared GNPs was added to 30 μL of 100 μM DNA3 solutions and the mixture was incubated for 16 h at room temperature, followed by addition of 0.2 mL of 2 M NaCl and incubation for another 24 h. Subsequently, the solution was further centrifuged at 16000 rpm for 15 min to remove the unbound DNA3. Finally, as-obtained DNA3-GNPs conjugations were rinsed and centrifuged twice, and re-dispersed in 600 μL of Tris–HCl buffer solution.

2.4. The aptasensor fabrication

Before modification, the cleaned Au electrode was placed into a thiolated DNA1 solution (5 μM in 50 mM Tris–HCl buffer) for 2 h to immobilize DNA1 at 37 °C, followed by treating with 0.5 mM MCH solution for 30 min. After washing with water, 5 μL of 5 μM DNA2 solution was placed on the electrode surface and the hybridization reaction was allowed to proceed for 1 h at 37 °C, DNA2/DNA1-Au was thus obtained. After rinsing and drying as above, DNA3-GNPs were then bound to the aptamer by placing 5 μL DNA3-GNPs suspension on the electrode surface at 37 °C for 1 h to obtain DNA3-GNPs/DNA2/DNA1-Au, followed by careful rinsing and drying treatment. Finally, 5 μL of 5 μM DNA4 was placed on the electrode surface at 37 °C to obtain the aptasensing interface (DNA4/DNA3-GNPs/DNA2/DNA1-Au). Prior to each analysis, the as-prepared electrode was immersed into OTA solutions with different concentrations for 15 min, followed by three rapid rinses with buffer solution. Next step, the electrode was immersed in MB solution (80 μM in 50 mM Tris–HCl) for 10 min followed by three rinses. Finally, the DPV responses were recorded in 50 mM Tris–HCl solution, which was purged with high-purity nitrogen for at least 15 min, at a scan rate of 4 mV s^{-1} and pulse amplitude of 50 mV.

3. Results and discussion

3.1. Conjugation of DNA3 to the gold nanoparticles

In the present work, DNA3 was conjugated on the surface of GNPs which was not only used as the first–level signal enhancer but also as the carrier of G–rich DNA to achieve the two–level signal amplification. Colloidal GNPs were synthesized by the trisodium citrate reduction method according to the previously published procedures. The presence of characteristic surface plasmon resonance (SPR) band at 522 nm in the UV-vis spectrum (curve a in Fig. 1A) confirmed the existence of the well-dispersed and spherical GNPs in aqueous solution. TEM micrograph image (Fig. 1B) showed that the resulting GNPs had a desirable dispersion of the spherical GNPs with an average diameter of 15 nm. For DNA strands couple, GNPs were treated with DNA3 to replace its original negative ions through the strong affinity of Au – S bonding. This replacement led to a slight shift of the SPR band, from 522 nm of GNPs to 525 nm of DNA3-GNPs (curve c in Fig. 1A), probably caused by the change in the dielectric constant of the DNA3 surrounding the GNPs. Intriguingly, there was no significant peak broadening suggested well dispersion of GNPs after being treated with DNA3. Compared with the spectrum of colloidal GNPs, an additional peak was observed at about 271 nm, similar to that of free DNA3 (curve b in Fig. 1A), indicating the successful immobilization of DNA3 on the surface of the GNPs.

Additionally, the concentration of DNA3-GNPs was calculated to be 10.5 nM according to the reported equation displayed as follows [41]:

$$c = N_{\text{total}}/NVN_{\text{A}} \quad (1)$$

where c is the concentration of DNA3-GNPs, N_{total} is the total numbers of gold atoms, N is the average number of gold atoms (N) for each GNP, V is the volume of DNA3-GNPs in liter, N_{A} is the Avogadro's constant. On the basis of the concentration of DNA3-GNPs and the amount of DNA3 used

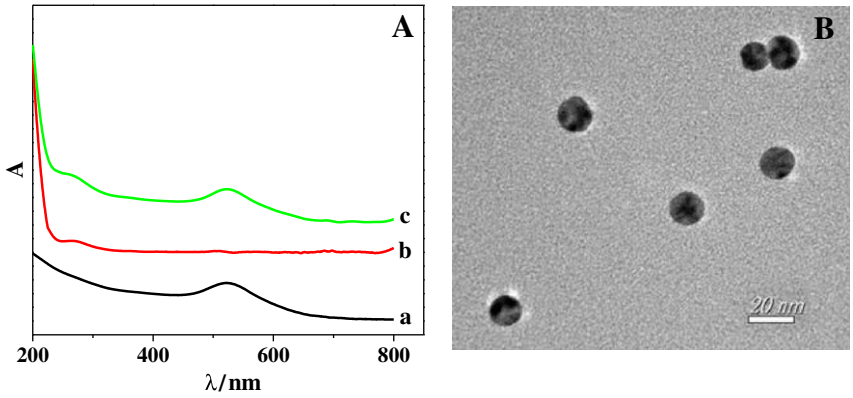

Fig. 1. (A) UV-vis spectra of GNPs (a), DNA3 (b), and DNA3-GNPs (c), and (B) TEM image of GNPs.

in the preparation process, the number of DNA3 on each GNP was estimated to be ~500 theoretically.

3.2. Aptasensor fabrication and detection principle

On the basis of the amplification effect of GNPs and the specific interaction between MB and free G bases in DNA strands, an amplified electrochemical sandwich detection strategy for OTA has been developed as illustrated in Scheme 1. Specifically, the surface of Au electrode was first modified with a thiolated DNA1. DNA2, the aptamer against OTA, was used as a bridge DNA that was immobilized on the electrode surface though partial hybridization with DNA1. DNA3-GNPs were then conjugated to the electrode surface through hybridization to the surface-confined aptamers, forming a sandwich structure of DNA3-GNPs/DNA2/DNA1-Au and achieving the first-level signal amplification of the peak current of MB. On the basis of this, the DNA4 designed with abundant G bases was bound to the GNPs surface through their partial hybridization with DNA3 on GNPs, providing vast anchoring sites for MB and achieving the second-level signal amplification. Since each GNP could be loaded with hundreds of DNA3 which brought hundreds of the G-rich DNA proximal to the electrode surface, this offered a significant amplification for the electrochemical signal. After the aptasensor (DNA4/DNA3-GNPs/DNA2/DNA1-Au) was successfully fabricated, the OTA solution was introduced to the detection system at different concentrations, and competed with DNA1 and DNA3 to form the OTA-aptamer complex. The more OTA molecules in the detection system, the more DNA2, DNA3-GNPs and DNA4 were dissociated from the sensing interface and thus changed the reduction current of MB. As a result, the decreased reduction current of MB was a direct function of the increased amounts of OTA in the tested solution. By employing this two-level cascaded signal amplification strategy, we demonstrated that this aptasensor could respond to a concentration of OTA as low as pM by using DPV measurements.

3.3. Characterization of the aptasensor fabrication

The aptasensor fabrication was verified by EIS measurements exploiting the solution-based redox probe $[Fe(CN)_6]^{3-/4-}$, which is very sensitive to monitor the changes in interfacial impedance upon DNA immobilization. A modified Randles' equivalent circuit (inset in Fig. 2A) was found to fit adequately the data over the entire measurement frequency range, where R_s and R_{ct} stood for the resistance of the electrolyte solution and charge transfer resistance, respectively; Z_W represented the Warburg impedance attributed to the contribution of diffusion, while Q represented the constant phase elements which were associated with the capacitance of the double layer. Throughout the

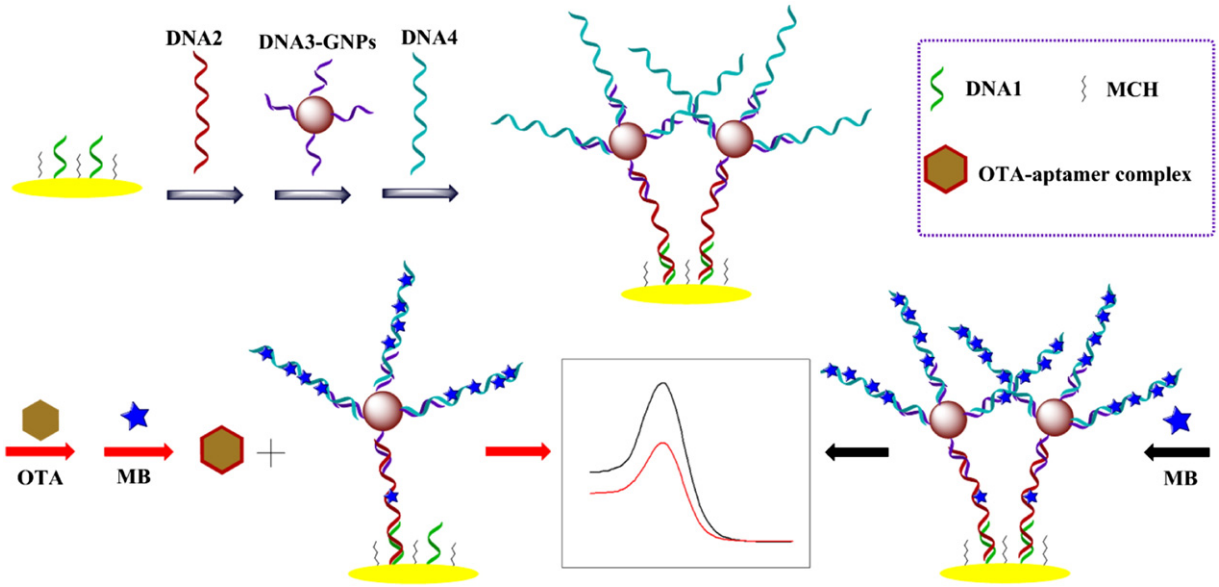

Scheme 1. Schematic representation of the electrochemical aptasensor designed for OTA detection.

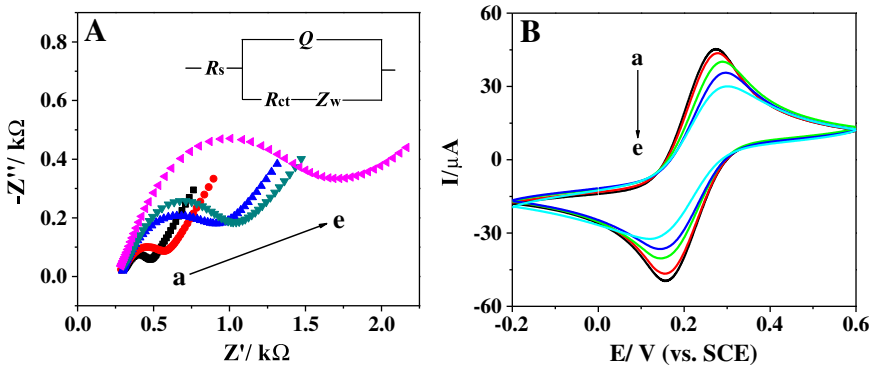

Fig. 2. EIS (A) and CV (B) response corresponding to different electrodes in 0.1 M KCl aqueous solution containing 5.0 mM $[Fe(CN)_6]^{3-/4-}$ (1:1, mole:mole). From a to e: bare Au electrode, DNA1-Au, DNA2/DNA1-Au, DNA3-GNPs/DNA2/DNA1-Au, DNA4/DNA3-GNPs/DNA2/DNA1-Au.

whole electrode modification processes, the changes in R_{ct} were the most significant among other impedance components and its value could be directly measured as the semicircle diameter observed at high frequencies in the impedance spectroscopy, which was thus a suitable signal for sensing the interfacial properties of the electrode surface.

The charge transfer process of $[Fe(CN)_6]^{3-/4-}$ at the bare electrode had a weak resistive force, so the bare Au electrode showed a very

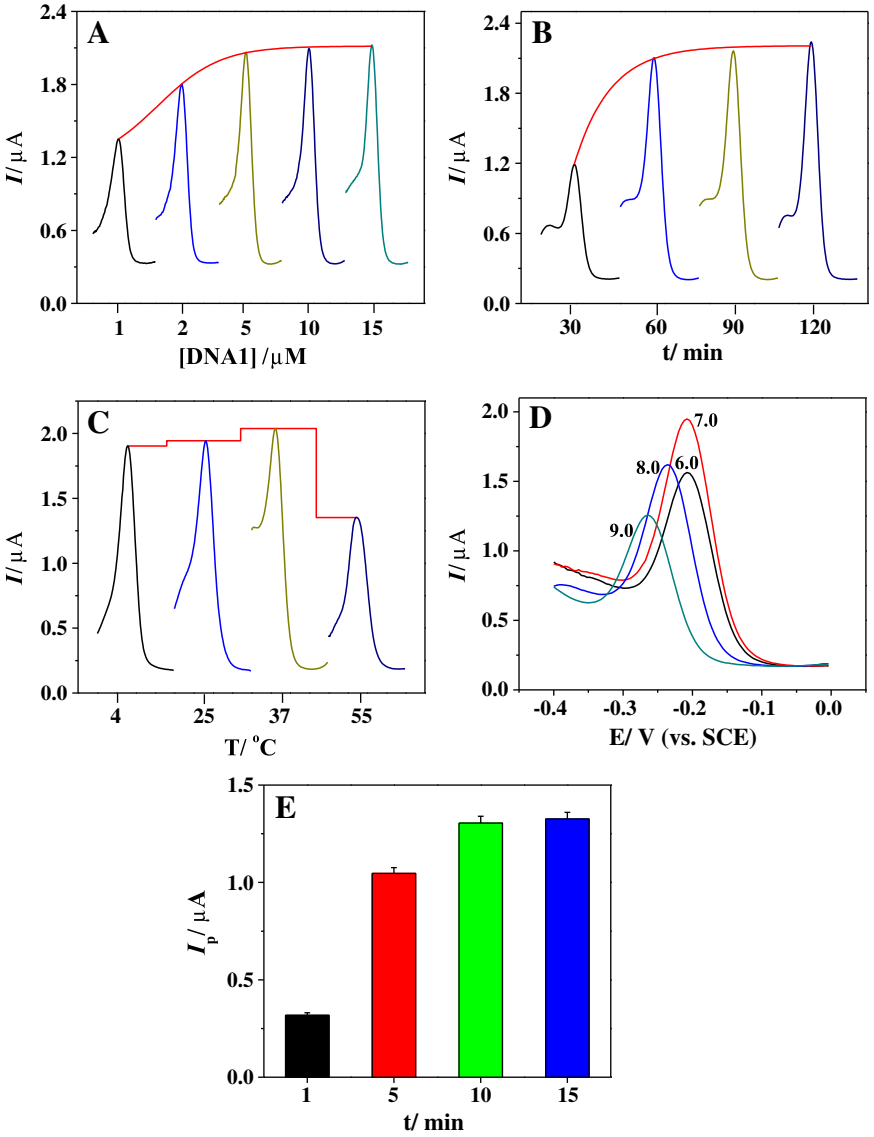

Fig. 3. DPV responses of the aptasensor under different detection factors: (A) DNA1 concentrations, (B) hybridization time, (C) the temperature, and (D) pH value of the detection system, (E) reaction time of the sensing interface with MB.

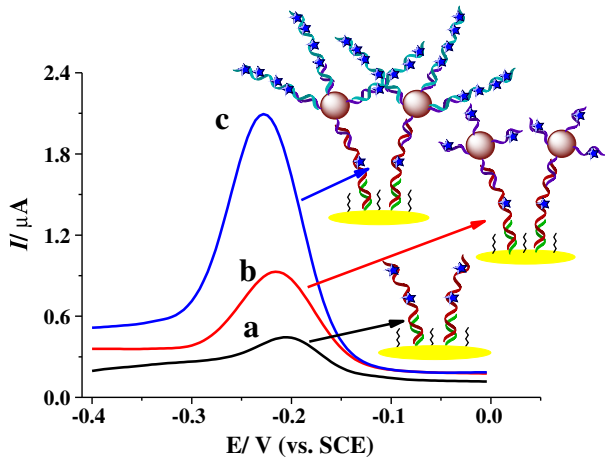

Fig. 4. DPV responses of DNA2/DNA1-Au (a), DNA3-GNPs/DNA2/DNA1-Au (b), and DNA4/DNA3-GNPs/DNA2/DNA1-Au (c).

small semicircle domain (curve a in Fig. 2A). When DNA1 was covalently immobilized on the Au electrode surface and then treated with MCH (curve b in Fig. 2A), an increase of the R_{ct} was observed as compared to the bare electrode, due to the repulsion between the negatively charged phosphate backbones of DNA1 and the negatively charged $[Fe(CN)_6]^{3-/4-}$, as well as the blocking effect of MCH. When DNA2 partially hybridized with DNA1, a half-duplex DNA structure was formed and more negatively charged phosphate backbones were introduced, leading to a further increase in R_{ct} (curve c in Fig. 2A). Although the GNPs have been loaded with a large number of DNA3, the R_{ct} value of DNA3-GNPs/DNA2/DNA1-Au increased slightly (curve d in Fig. 2A), which mainly attributed to the significantly improved electrical conductivity of GNPs. When DNA4 was introduced onto the electrode surface (curve e in Fig. 2A), the R_{ct} value dramatically increased as compared to that of the DNA3-GNPs/DNA2/DNA1-Au. This was largely attributed to the fact that the GNPs surface had been coated with a large number of DNA4 molecules. The resulting coat contained more negatively charged phosphate backbones which prevented $[Fe(CN)_6]^{3-/4-}$ from reaching the electrode, suggesting the successful immobilization of DNA4 through their partial hybridization with DNA3. The corresponding CVs characterizations are also shown in Fig. 2B. The peak currents decreased and the peak-to-peak separation increased along with the aptasensor fabrication process, which was in good agreement with that of EIS studies.

3.4. The optimization of important factors

To generate a rapid-response method with low detection limit for OTA detection, it is significant to optimize different parameters involved in the sensor fabrication and detection process. The DPV response obtained from the aptasensor was mainly due to the amount of GNPs and free G-bases in DNA4 which were dependent on the immobilization of DNA1. As shown in Fig. 3A, the peak current increased dramatically with DNA1 concentration increasing from 1 to 5 μM, and the peak current intensity tended to be stable beyond 5 μM. Therefore, 5 μM was the saturated concentration of DNA1 and was selected to be the optimized concentration of DNA1. As the molar ratio of hybridization between two complementary ssDNA is 1, it is reasonable to choose 5 μM as the suitable concentration of the DNA2 for the following study. Because DNA hybridization is a time-dependent process, the hybridization time between DNA1 and DNA2 was also optimized. Following the routine hybridization times, from 10 to 120 min were studied as displayed in Fig. 3B. The peak current increased dramatically with the growth of the time before 60 min, and then leveled off at times longer than 60 min, so 60 min was used as the time required for hybridization of DNA1 and DNA2, and also for subsequent DNA hybridization. Another important factor that affected DNA hybridization was the temperature of buffer solution. Fig. 3C showed that the peak current reached the maximal intensity when temperature was 37 °C, which was then used for subsequent detection. The reduction reaction of MB was influenced by the pH value of the supporting electrolyte. Based on physiological conditions, pH values from 6.0 to 9.0 were tested and the results shown in Fig. 3D suggested the best performance was obtained in the Tris–HCl buffer solution with a pH value of 7.0. Besides, accumulation time of MB could also influence the responses of the aptasensor. Fig. 3E revealed that the peak current rose with the increase of time from 1 to 10 min and ceased to increase beyond 10 min. Form this regard, 10 min was then selected as the reaction time between the sensing interface with MB molecules. Additionally, the stability of MB on the sensing interface was also investigated. It was found that the signal intensity declined to 84.3% of the original reduction peak after three repetitive measurements. Therefore, all the exhibited DPV signals were recorded from the first scanning.

3.5. Two-level cascaded signal amplification strategy based on GNPs and G-rich DNA

After the accumulation of MB, the sandwich DNA complex on the electrode surface led to an electrocatalytic current from the surface-immobilized MB, measured by the DPV technique (Fig. 4). In the absence of the first-level signal amplification of GNPs, only a slight increase in the peak current was observed for DNA2/DNA1-Au (curve a), coming from the adsorbed MB by the specific interaction between a minimum of free G bases present in DNA2. When DNA3-GNPs were hybridized to the electrode (curve b), a larger reduction peak appeared, ~3.4 (±0.3) times higher than that of the DNA2/DNA1–Au electrode without the DNA3-GNPs, confirmed the signal amplification feature of GNPs as previous reports [38,42]. However, the signal amplification

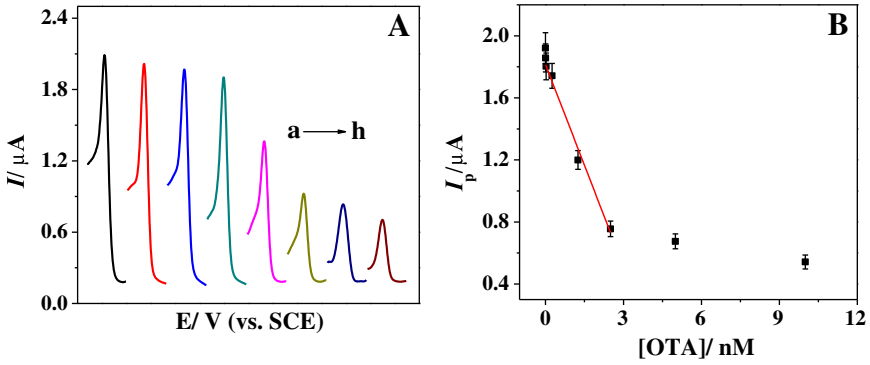

Fig. 5. (A) DPV responses of the aptasensor at different OTA concentrations, from a to h: 0, 2.5×10^{-3}, 2.5×10^{-2}, 0.25, 1.25, 2.5, 5.0, and 10.0 nM. (B) Calibration plot of peak current vs. OTA concentration, and calibration Eq. (1) is shown in the text.

based on the DNA3 functionalized GNPs is not sufficient for the ultrasensitive aptasensor. As reported by Kerman et al. [43], MB is easy to anchor on DNA modified electrode by the interaction between MB and free G bases. As a result, a G-rich DNA containing 25 G bases was designed to provide abundant anchoring sits for MB to achieve the more sensitive OTA detection. It was reasonable that a larger reduction peak of MB was observed at DNA4/DNA3-GNPs/DNA2/DNA1-Au (curve c) with a larger number of free G bases to bind with MB. The peak current of MB was ~2.5 (±0.2) fold higher than the first-level signal amplification from GNPs, confirming the formation of the second-level signal amplification. Therefore, both the amplification effect of GNPs and the abundant free G bases on DNA4 played important roles in the dramatic increase of peak current. With the help of the two-level cascaded signal amplification, the DPV response of the DNA4/DNA3-GNPs/DNA2/DNA1 modified electrode was ~8.5 (±0.3) fold higher than that of the DNA2/DNA1 modified electrode, implying that one could use this two-level cascaded signal amplification strategy to realize OTA detection with ultrahigh sensitivity.

3.6. Ultrasensitive electrochemical detection of OTA

When the aptasensor was immersed into the OTA-containing solution, the formation of the OTA–aptamer complex resulted in the detachment of DNA3-GNPs and DNA4 into bulk solution along with the aptamer desorption from the capture probe, which caused a peak current decrease of MB. On the basis of these findings, the amplified aptasensor was used for OTA detection under the optimized experimental conditions. The results showed that the reduction peak intensity (I_p) of MB decreased as the concentration of OTA increased in the tested solution (Fig. 5A). By analyzing the I_p with the concentrations of OTA, the linear curve of I_p vs. [OTA] (Fig. 5B) was fitted to a regression equation as follows:

$$I_p(\mu A) = (-0.433 \pm 0.029)[\mathrm{OTA}](\mathrm{nM}) + (1.815 \pm 0.048)(R = 0.994) \quad (2)$$

With signal enhancement from the dual signal enhancer, the effective sensing range was from 2.5 pM to 2.5 nM with an extremely low detection limit of 0.75 (±0.12) pM which was approximately ~1000 fold lower than that of most other existing electrochemical aptasensors down to ~nM, for example, 0.25 nM [30] and 0.28 nM [33]. The sensitivity of our proposed sensing system for OTA was calculated to be 0.47 (±0.04) μA nM^{-1}. These results demonstrated that the proposed aptasensor are highly sensitive, especially for the detection of OTA at low levels. Nevertheless, the linear range of the aptasensor was not very broad, which might be attributed to a small amount of DNA2 assembled on the electrode surface resulting from a short reaction time (2 h) between the Au electrode and DNA1.

The selectivity of aptasensor was evaluated by the comparison of the sensing results of FB1, OTB, and OTA at the same concentration of 2.5 nM. As shown in Table 1, the response signals to FB1 and OTB were neglectable while an obvious decrease in response was observed for OTA, attributing to the specific recognition force of aptamer to OTA [40], which suggested that the aptasensor possessed high selectivity. The reproducibility of the aptasensor was studied at the OTA concentration of 0.25 nM, and the relative standard deviation (RSD) for five times was 4.9%. In addition, five freshly prepared aptasensors have been used for the detection of OTA with the same concentration of 0.25 nM. All the aptasensor exhibited similar DPV response and a RSD of 7.1% was obtained, indicating that the designed aptasensor for OTA detection was highly reproducible.

Table 1
DPV response of the aptasensor incubated with different targets.

Targets	I_p/μA
No	1.92 ± 0.09
FB1	1.90 ± 0.08
OTB	1.89 ± 0.08
OTA	0.76 ± 0.05

Table 2
Results of OTA detection in red wine samples.

Added/nM	Found/nM	RSD/%	Recovery/%
0.125	0.113	7.4	90
0.25	0.233	5.2	93
1.25	1.187	5.9	95

3.7. Detection of OTA in red wine samples

The performance of as-prepared aptasensor was measured by studying the recovery of the sensor. The red wine samples without OTA purchased from the local supermarket were subjected to a simple pretreatment process according to the reported method [36]. After filtrating, the solution was adjusted to pH 7.0 and diluted ~10 fold for later use. The recovery experiment was carried out by reacting with five levels of standard real samples which were prepared by spiking five different standard concentrations of OTA standard solution. As can seen from Table 2, the recovery and RSD values were acceptable, demonstrating the aptasensor had a promising feature for the practical use in red wine samples.

4. Conclusions

In summary, an ultrasensitive electrochemical method for OTA detection was developed based on two-level cascaded signal amplification strategy through the aptamer-based sandwich model. With the help of the dual signal enhancer, the DPV response of the aptasensor was ~8.5 (±0.3) fold higher than that of the GNPs/G-rich DNA absence. On the basis of these findings, an ultrasensitive electrochemical aptasensor was fabricated and showed a decreased response to the increase of OTA concentration with an extremely low detection limit. Additionally, the as-prepared aptasensor possessed good selectivity and reproducibility and could be successfully used to detect OTA in real wine samples. As the GNPs can be functionalized with other reporter DNA and the G-rich DNA can be designed in desire and labeled with other signal probes, the aptasensor developed here provides a promising signal amplified model for small molecules, proteins, and cells detection with even other techniques.

Acknowledgements

The present work was supported by the National Natural Science Foundation of China (No. 21175061 and 21375050), the Natural Science Foundation of Jiangsu province (No. BK20130481), China Postdoctoral Science Foundation (No. 2012M520998), major Program of Natural Science Foundation of Education Bureau of Jiangsu Province, China (Grant No. 340 10KJA470007), Key Laboratory of Modern Agriculture Equipment and Technology 341 (No. NZ201109), Jiangsu Planned Projects for Postdoctoral Research Funds (1301141C), and Research Foundation of Jiangsu University (12JDG087).

References

[1] S. Amézqueta, E. González–Peñas, M. Murillo–Arbizu, A.L. Cerain, Ochratoxin A decontamination: a review, Food Control 20 (2009) 326–333.
[2] A.A. Ansari, A. Kaushik, P.R. Solanki, B.D. Malhotra, Nanostructured zinc oxide platform for mycotoxin detection, Bioelectrochemistry 77 (2010) 75–81.
[3] I. Barna-Vetro, L. Solti, J. Teren, A. Gyongyosi, E. Szabo, A. Wolfing, Sensitive ELISA test for determination of ochratoxin A, J. Agric. Food Chem. 44 (1996) 4071–4074.
[4] A.D. Girolamo, M. McKeague, J.D. Miller, M.C. DeRosa, A. Viscon, Determination of ochratoxin A in wheat after clean-up through a DNA aptamer-based solid phase extraction column, Food Chem. 127 (2011) 1378–1384.

[5] J. Blesa, J.M. Soriano, J.C. Moltó, J. Mañes, Concentration of ochratoxin A in wines from supermarkets and stores of Valencian Community (Spain), J. Chromatogr. A 1054 (2004) 397–401.
[6] J.H. Chen, Z.Y. Fang, J. Liu, L.W. Zeng, A simple and rapid biosensor for ochratoxin A based on a structure-switching, Food Control 25 (2012) 555–560.
[7] N. Duan, S.J. Wu, Z.P. Wang, An aptamer-based fluorescence assay for ochratoxin A, Chin. J. Anal. Chem. 39 (2011) 300–304.
[8] C. Yang, V. Lates, B. Prieto–Simón, J.L. Marty, X.R. Yang, Aptamer-DNAzyme hairpins for biosensing of ochratoxin A, Biosens. Bioelectron. 32 (2012) 208–212.
[9] P. Songsermsakul, E. Razzazi–Fazelib, A review of recent trends in applications of liquid chromatography–mass spectrometry for determination of mycotoxins, J. Liq. Chromatogr. Relat. Technol. 31 (2008) 1641–1686.
[10] N.W. Turner, S. Subrahmanyam, S.A. Piletsky, Analytical methods for determination of mycotoxins: a review, Anal. Chim. Acta. 632 (2009) 168–180.
[11] C. Tessini, C. Mardones, D. von Baer, M. Vega, E. Herlitz, R. Saelzer, J. Silva, O. Torres, Alternatives for sample pre-treatment and HPLC determination of ochratoxin A in red wine using fluorescence detection, Anal. Chim. Acta. 660 (2010) 119–126.
[12] F.Y. Yu, T.F. Chi, B.H. Liu, C.C. Su, Development of a sensitive enzyme-linked immunosorbent assay for the determination of ochratoxin A, J. Agric. Food Chem. 53 (2005) 6947–6953.
[13] F.Y. Yu, M.M. Vdovenko, J.J. Wang, I.Y. Sakharov, Comparison of enzyme-linked immunosorbent assays with chemiluminescent and colorimetric detection for the determination of ochratoxin A in food, J. Agric. Food Chem. 59 (2011) 809–813.
[14] B. Prieto–Simon, M. Campas, J.L. Marty, T. Noguer, Novel highly–performing immunosensor based strategy for ochratoxin A detection in wine samples, Biosens. Bioelectron. 23 (2008) 995–1002.
[15] D.R. Shankaran, K.V. Gobi, N. Miura, Recent advancements in surface plasmon resonance immunosensors for detection of small molecules of biomedical, food and environmental interest, *Sensor. Actuat. B-Chem.* 121 (2007) 158–177.
[16] N.E. Ahmed, M.M. Farag, K.M. Soliman, A.K.M. Abdel–Samed, K.M. Naguib, Evaluation of methods used to determine ochratoxin A in coffee beans, J. Agric. Food Chem. 55 (2007) 9576–9580.
[17] B.H. Liu, Z.J. Tsao, J.J. Wang, F.Y. Yu, Development of a monoclonal antibody against ochratoxin A and its application in enzyme-linked immunosorbent assay and gold nanoparticle immunochromatographic strip, Anal. Chem. 80 (2008) 7029–7035.
[18] F. Zezza, F. Longobardi, M. Pascale, S.A. Eremin, A. Visconti, Fluorescence polarization immunoassay for rapid screening of ochratoxin A in red wine, Anal. Bioanal. Chem. 395 (2009) 1317–1323.
[19] A. Rhouatia, A. Hayat, D.B. Hernandez, Z. Meraihi, R. Munoz, J.L. Marty, Development of an automated flow-based electrochemical aptasensor for on–line detection of ochratoxin A, *Sensor. Actuat. B-Chem.* 176 (2013) 1160–1166.
[20] R. Stoltenburg, C. Reinemann, B. Strehlitz, SELEX–a revolutionary method to generate high-affinity nucleic acid ligands, Biomol. Eng. 24 (2007) 381–403.
[21] N.B. Sankaran, S. Nishizawa, T. Seino, K. Yoshimoto, N. Teramae, Abasic-site-containing oligodeoxynucleotides as aptamers for riboflavin, Angew. Chem. Int. Ed. 45 (2006) 1563–1568.
[22] D. Shangguan, Y. Li, Z. Tang, Z.C. Cao, H.W. Chen, P. Mallikaratchy, K. Sefah, C.J. Yang, W. Tan, Aptamers evolved from live cells as effective molecular probes for cancer study, Proc. Natl. Acad. Sci. U. S. A. 103 (2006) 11838–11843.
[23] A.K.H. Cheng, D. Sen, H.Z. Yu, Design and testing of aptamer-based electrochemical biosensors for proteins and small molecules, Bioelectrochemistry 77 (2009) 1–12.
[24] T. Mairal, V.C. Özalp, P.L. Sánchez, M. Mir, I. Katakis, C.K. O'Sullivan, Aptamers: molecular tools for analytical applications, Anal. Bioanal. Chem. 390 (2008) 989–1007.
[25] J.A. Cruz–Aguado, G. Penner, Determination of ochratoxin A with a DNA aptamer, J. Agric. Food Chem. 56 (2008) 10456–10461.
[26] Z.J. Guo, J.T. Ren, J.H. Wang, E.K. Wang, Single-walled carbon nanotubes based quenching of free FAM-aptamer for selective determination of ochratoxin A, Talanta 85 (2011) 2517–2521.
[27] L. Sheng, J. Ren, Y. Miao, J. Wang, E. Wang, PVP-coated graphene oxide for selective determination of ochratoxin A via quenching fluorescence of free aptamer, Biosens. Bioelectron. 26 (2011) 3494–3499.
[28] A.D. Girolamo, L. Le, G. Penner, R. Schena, A. Visconti, Analytical performances of a DNA–ligand system using time-resolved fluorescence for the determination of ochratoxin A in wheat, Anal. Bioanal. Chem. 403 (2012) 2627–2634.
[29] Z. Wang, N. Duan, X. Hun, S. Wu, Electrochemiluminescent aptamer biosensor for the determination of ochratoxin A at a gold-nanoparticles modified gold electrode using N-(aminobutyl)-N-ethylisoluminol as a luminescent label, Anal. Bioanal. Chem. 398 (2010) 2125–2132.
[30] P. Prabhakar, Z. Matharu, B.D. Malhotra, Polyaniline Langmuir–Blodgett film based aptasensor for ochratoxin A detection, Biosens. Bioelectron. 26 (2011) 4006–4011.
[31] J.J. Wu, H.Q. Chu, Z.L. Mei, Y. Deng, F. Xue, L. Zheng, W. Chen, Ultrasensitive one-step rapid detection of ochratoxin A by the folding-based electro chemical aptasensor, Anal. Chim. Acta. 753 (2012) 27–31.
[32] P. Tong, L. Zhang, J.J. Xu, H.Y. Chen, Simply amplified electrochemical aptasensor of ochratoxin A based on exonuclease-catalyzed target recycling, Biosens. Bioelectron. 29 (2011) 97–101.
[33] L. Bonel, J.C. Vidal, P. Duato, J.R. Castillo, An electrochemical competitive biosensor for ochratoxin A based on a DNA biotinylated aptamer, Biosens. Bioelectron. 26 (2011) 3254–3259.
[34] L. Barthelmebs, A. Hayat, A.W. Limiadi, J.L. Marty, T. Noguer, Electrochemical DNA aptamer-based biosensor for OTA detection using superparamagnetic nanoparticles, *Sensor. Actuat. B-Chem.* 156 (2011) 932–937.
[35] P. Tong, W.W. Zhao, L. Zhang, J.J. Xu, H.Y. Chen, Double-probe signal enhancing strategy for toxin aptasensing based on rolling circle amplification, Biosens. Bioelectron. 33 (2012) 146–151.
[36] W. Ma, H.H. Yin, L.G. Xu, Z. Xu, H. Kuang, L.B. Wang, C.L. Xu, Femtogram ultrasensitive aptasensor for the detection of ochratoxin A, Biosens. Bioelectron. 42 (2013) 545–549.
[37] L. Huang, J.J. Wu, L. Zheng, H.S. Qian, F. Xue, Y.C. Wu, D.D. Pan, S.B. Adeloju, W. Chen, Rolling chain amplification (RCA) based signal enhanced electrochemical aptasensor for rapid and ultrasensitive detection of ochratoxin A, Anal. Chem. 85 (2013) 10842–10849.
[38] H. Kuang, W. Chen, D.H. Xu, L.G. Xu, Y.Y. Zhu, L.Q. Liu, H.Q. Chu, C.F. Peng, C.L. Xu, S.F. Zhu, Fabricated aptamer-based electrochemical "signal-off" sensor of ochratoxin A, Biosens. Bioelectron. 26 (2010) 710–716.
[39] P. Kara, K. Kerman, D. Ozkan, B. Meric, A. Erdem, Z. Ozkan, M. Ozsoz, Electrochemical genosensor for the detection of interaction between methylene blue and DNA, Electrochem. Commun. 4 (2002) 705–709.
[40] J.L. Wang, F. Wang, S.J. Dong, Methylene blue as an indicator for sensitive electrochemical detection of adenosine based on aptamer switch, J. Electroanal. Chem. 626 (2009) 1–5.
[41] X. Liu, M. Atwater, J.H. Wang, Q. Huo, Extinction coefficient of gold nanoparticles with different sizes and different capping ligands, Colloids Surf. B 58 (2007) 3–7.
[42] J. Zhang, S.P. Song, L.Y. Zhang, L.H. Wang, H.P. Wu, D. Pan, C.H. Fan, Sequence-specific detection of femtomolar DNA via a chronocoulometric DNA sensor (CDS): effects of nanoparticle-mediated amplification and nanoscale control of DNA assembly at electrodes, J. Am. Chem. Soc. 128 (2006) 8575–8580.
[43] K. Kerman, D. Ozkan, P. Kara, B. Meric, J.J. Gooding, M. Ozsoz, Voltammetric determination of DNA hybridization using methylene blue and self-assembled alkanethiol monolayer on gold electrodes, Anal. Chim. Acta. 462 (2002) 39–47.